

Blood Bacterial Profiles Associated With Human Immunodeficiency Virus Infection and Immune Recovery

Sergio Serrano-Villar,¹ Sergio Sanchez-Carrillo,² Alba Talavera-Rodríguez,³ Benjamin Lelouvier,⁴ Carolina Gutiérrez,¹ Alejandro Vallejo,¹ Florence Servant,⁴ José I. Bernadino,⁵ Vicente Estrada,⁶ Nadia Madrid,¹ María José Gosalbes,^{7,8} Otilia Bisbal,⁹ María de Lagarde,⁹ Javier Martínez-Sanz,¹ Raquel Ron,¹ Sabina Herrera,¹ Santiago Moreno,¹ and Manuel Ferrer²

¹Department of Infectious Diseases, Hospital Universitario Ramón y Cajal, Facultad de Medicina, Universidad de Alcalá, Instituto de Investigación Sanitaria Ramón y Cajal, Madrid, Spain, ²Institute of Catalysis, Consejo Superior de Investigaciones Científicas, Madrid, Spain, ³Bioinformatics Unit, Hospital Universitario Ramón y Cajal, Facultad de Medicina, Universidad de Alcalá, Instituto de Investigación Sanitaria Ramón y Cajal, Madrid, Spain, ⁴Vaiomer, Labège, France, ⁵HIV Unit, Hospital Universitario La Paz, Madrid, Spain, ⁶HIV Unit, Hospital Clínico San Carlos, Madrid, Spain, ⁷Area of Genomics and Health, FISABIO-Salud Pública, Valencia, Spain, ⁸CIBER Epidemiología y Salud Pública, Madrid, Spain, and ⁹HIV Unit, Hospital Universitario Doce de Octubre, Madrid, Spain

Human immunodeficiency virus (HIV) infection impairs mucosal immunity and leads to bacterial translocation, fueling chronic inflammation and disease progression. While this is well established, questions remain about the compositional profile of the translocated bacteria, and to what extent it is influenced by antiretroviral therapy (ART). Using 16S ribosomal DNA targeted sequencing and shotgun proteomics, we showed that HIV increases bacterial translocation from the gut to the blood. HIV increased alpha diversity in the blood, which was dominated by aerobic bacteria belonging to Micrococcaceae (Actinobacteria) and Pseudomonadaceae (Proteobacteria) families, and the number of circulating bacterial proteins was also increased. Forty-eight weeks of ART attenuated this phenomenon. We found that enrichment with Lactobacillales order, and depletion of Actinobacteria class and Moraxellaceae and Corynebacteriaceae families, were significantly associated with greater immune recovery and correlated with several inflammatory markers. Our findings suggest that the molecular cross talk between the host and the translocated bacterial products could influence ART-mediated immune recovery.

Keywords. HIV; microbiota; CD4 T cells; immunoactivation; inflammation.

A hallmark feature of human immunodeficiency virus (HIV) and simian immunodeficiency virus (SIV) infection is a rapid impairment in the gut-associated lymphoid tissue (GALT), which allows translocation of microbial products into the bloodstream [1–5] and triggers innate and adaptive immune responses. During treatment of HIV infection, the immunological and structural defects in the GALT are only partially restored [6]. These abnormalities allow for increased bacterial translocation, and there are now overwhelming evidences indicating that these drive inflammation and adverse clinical outcomes [7–10]. The extent of antiretroviral therapy (ART)-mediated immune recovery in the peripheral blood correlates with impaired epithelial proliferation, increased neutrophil infiltration, and mucosal apoptosis in colorectal biopsy specimens [6, 9], which is probably influenced by the decrease in the number of T cells that are trafficking to the gut [3, 11]. These abnormalities will arguably have consequences on the signals that are required for

the coordination of commensal colonization, which could explain the shifts in microbial distributions and metabolic activity of the gut microbial communities [12–15]. Notably, microbial translocation does not seem to occur in “natural host” species, such as African green monkeys and sooty mangabeys, in which SIV infection is nonpathogenic [16, 17].

A number of recent sequence-based and ultramicroscopic studies have uncovered a blood bacterial DNA profile in several noncommunicable diseases [18]. Whether HIV infection is associated with a specific microbial signature in peripheral blood, the possible links between the identity of the translocated bacteria, and the extent of immunological recovery during ART remain unknown.

METHODS

Study Design, Participants, Setting, and Eligibility

We conducted a cohort study. Participants were HIV-infected late-presenting (CD4⁺ T-cell count <350/μL or AIDS at diagnosis [19]) adults who were started on ART, according to the Spanish Grupo de Estudio del SIDA National Guidelines [20, p 143] and who were followed up for 48 weeks. Controls were recruited from healthy non-HIV-infected individuals who accompanied the patients to the clinics, medical students, or hospital staff, with the goal of achieving a group with a similar age. The study was approved by the ethics committee at all participating centers, and all participants signed an informed consent before initiation of study procedures.

Received 27 February 2020; editorial decision 19 June 2020; accepted 23 June 2020; published online June 30, 2020.

Presented in part: HIV and Microbiome Workshop, Rockville, Maryland, 19–20 October 2017; Conference of Retrovirus and Opportunistic Infections, Seattle, Washington, 4–7 March 2019.

Correspondence: Sergio Serrano-Villar, Department of Infectious Diseases, Hospital Universitario Ramón y Cajal, Facultad de Medicina, Universidad de Alcalá (IRYCIS). Carretera de Colmenar Viejo, Km 9.100, 28034 Madrid, Spain (sergio.serrano@salud.madrid.org).

The Journal of Infectious Diseases® 2021;223:471–81

© The Author(s) 2020. Published by Oxford University Press for the Infectious Diseases Society of America. All rights reserved. For permissions, e-mail: journals.permissions@oup.com. DOI: 10.1093/infdis/jiaa379

Metagenomic Sequencing of Blood Samples and Contaminant Control

DNA from blood samples was isolated and amplified in a strictly controlled environment at Vaiomer a biotech company and contract research organization (CRO) expert in tissue and blood microbiota, using a stringent contamination-aware approach described and discussed elsewhere [21]. For each patient, 10–20 mL of whole blood was collected in ethylenediaminetetraacetic acid tubes. The high volume of blood withdrawn prevents any significant impact on the results of contamination by skin microbiome and clinical setup environment, as discussed and tested previously [22–24].

DNA Extraction

Total DNA was extracted from 100 μ L of whole blood using a specific Vaiomer protocol carefully designed to minimize any risk of contamination between samples or from the experimenters, environment, as described elsewhere [22]. The quality and quantity of extracted nucleic acids were controlled by means of gel electrophoresis (1% [wt/wt] agarose in 0.53 mol/L Tris/borate/ethylenediaminetetraacetic acid) and a NanoDrop 2000 UV spectrophotometer (Thermo Scientific).

Library Construction and Sequencing

Because many reagents that are required for quantitative polymerase chain reaction (qPCR) and the sequencing pipeline contain nonnegligible amounts of bacterial DNA [25, 26], we tested numerous combinations of reagents to minimize bacterial contaminants and adapted the protocol to increase the yield of amplified bacterial DNA that was present in the blood. The methods have been described in detail elsewhere [21, 22]. PCR amplification was performed using 16S ribosomal RNA gene universal primers that targeted the hypervariable regions of 16S ribosomal DNA (rDNA) and that were amplified. The amplicon length was set to encompass the 467 base pairs (in *Escherichia coli* reference genome) using the 2 \times 300 paired-end MiSeq kit v3. For each sample, a sequencing library was generated by adding sequencing adapters. The detection of the sequencing fragments was performed using MiSeq Illumina technology. To quantify the number of 16S rDNA copies per milliliter of plasma, the absolute copy number was determined using a previously published universal 16S rDNA qPCR assay [27].

To ensure a low background signal from bacterial contamination of reagents and consumables, in addition to blood samples, 2 types of negative controls consisting of molecular grade water were added in an empty tube separately at the DNA extraction step and the PCR steps and were amplified and sequenced at the same time as the extracted DNA of the blood samples to ensure a low background signal from bacterial contamination of reagents and consumables. Bacterial DNA concentrations assessed by qPCR (Figure 1A), alpha diversity analysis (Figure 1B) and beta diversity analysis (Figure 1C) all show a clear separation between both

negative controls and blood samples. These controls confirm that bacterial contamination is well contained in our pipeline and has a negligible impact on the taxonomic profiles of the samples of this study, as reported elsewhere [21–24].

Bioinformatics Pipeline

16S rDNA amplicons were clustered into operational taxonomic units before taxonomic assignment, as described elsewhere [21, 22]. The targeted metagenomic sequences from microbiota were processed using the bioinformatics pipeline that was established by Vaiomer based on the Find Rapidly OTU with Galaxy Solution guidelines [28]. Briefly, after demultiplexing of the bar-coded Illumina paired reads, single read sequences were independently cleaned and paired for each sample into longer fragments. Operational taxonomic units were produced via single-linkage clustering, and taxonomic assignments were performed to determine community profiles.

Blood Protein Analysis

Protein samples from whole blood were collected and analyzed with a proteomic approach using a pooling strategy, successfully used to identify proteomic biomarkers [29]. Pooling increased the protein amount, which is low in individual blood samples, while reducing the number of samples through the analysis of 2 pools each containing approximately half of the individuals. Two pools of 7 and 8 samples in HIV-infected pre-ART and HIV-infected post-ART groups of individuals were created, and 2 pools of 10 samples each in the healthy controls. In all cases, whole blood samples were thawed on the day of the experiment, and 100 μ L was subjected to immunoaffinity extraction, as described elsewhere [30].

Protein samples were combined to yield 1 μ g of total protein each per pool, which were subjected to tryptic digestion, followed by 1D-nano liquid chromatography electrospray ionization tandem mass spectrometric analysis, data analysis, and protein expression level by means of the exponentially modified protein abundance index, as described elsewhere [29]. Paired 2-sample *t* tests were used for pairwise comparisons of the relative abundance of proteins of interest (IBM SPSS Statistics, version 20.01 IBM). The mass spectrometry proteomics data have been deposited to the ProteomeXchange Consortium via the PRIDE [1] partner repository, with the data set identifiers PXD017484 and 10.6019/PXD017484.

The **Supplementary Materials** include a detailed description of the methods used for measuring plasma bacterial proteins, inflammatory biomarkers (high-sensitivity C-reactive protein, soluble CD163, interleukin 6, 7, 10, and 17A, CXCL10, and tumor necrosis factor α), and bacterial translocation markers (soluble CD14 and lipoteichoic acid), and for T-cell immunophenotyping, blood protein analysis, 16S ribosomal RNA gene sequencing, and bioinformatics analysis of fecal samples, along with the statistical analysis.

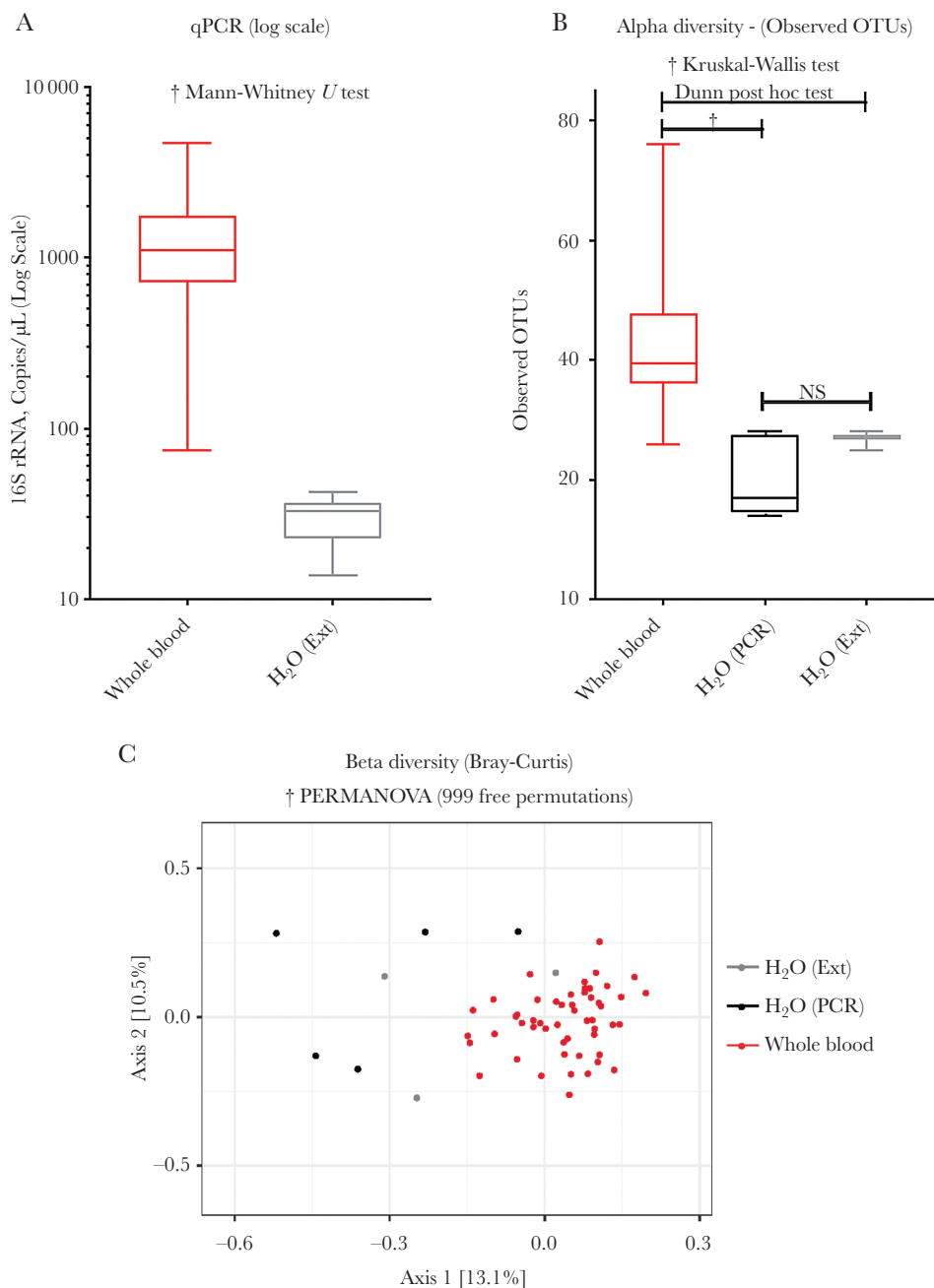


Figure 1. *A*, Quantitative polymerase chain reaction (qPCR)-based 16S ribosomal RNA (rRNA) gene abundance is significantly higher in whole-blood samples than in negative controls, based on Mann-Whitney *U* tests. *B*, Whole-blood samples exhibit significantly higher operational taxonomic unit (OTU) richness than negative controls, based on Kruskal-Wallis followed by Dunn post hoc tests. In box plots in *A* and *B*, the horizontal line represents the median; the lower portion of the box, the 25th percentile; the upper portion, the 75th percentile; and the whiskers, the minimum and maximum values. *C*, Ordination of 16S rRNA gene sequencing data using Bray-Curtis dissimilarity measure shows clear separation of whole-blood samples from negative controls. Abbreviations: H₂O (Ext) molecular grade water added in an empty tube, extracted, and analyzed (with qPCR and/or sequencing) at the same time as the samples (as negative control); H₂O (PCR), molecular grade water added in an empty tube, amplified, and sequenced at the same time as the extracted DNA of the samples (negative control); NS, not significant; PERMANOVA, permutational multivariate analysis of variance. **P* < .01; †*P* < .001.

RESULTS

General Characteristics of the Study Population

We included 30 HIV-infected participants and 20 healthy controls (Table 1). All HIV-infected participants who started triple ART completed the 48-week follow-up. Their mean age was 38 years, 91% were male, and 83% were men who have

sex with men. The median CD4⁺ T-cell counts were 225/ μ L (IQR, 117–288/ μ L), and the median CD4/CD8 ratio was 0.27 (0.13–0.34). HIV-infected individuals did not show different dietary habits compared with controls (Supplementary Figure 1). We detected significant differences only in the median vegetable consumption, with a median of 10 servings

Table 1. Baseline Characteristics of the Study Population

Characteristic	Controls (n = 20)	HIV-Infected Participants (n = 30)	INRs (n = 15)	IRs (n = 15)	PValue (INRs vs IRs)
Age, mean (SD), y	39.1 (11.9)	39.9 (12.4)	41.9 (10.8)	37.9 (13.9)	.19
Male, no. (%)	15 (75)	27 (90)	14 (93.4)	13 (86.7)	.54
BMI, mean (SD) ^a	23.7 (4.2)	23.2 (3.2)	23.2 (3.3)	23.2 (3.2)	.79
Time since HIV diagnosis, median (IQR), months	...	3.3 (0.8–18.5)	3.7 (0.8–26.3)	2.6 (1.2–6.2)	.70
Risk factor, no. (%)					
IDU	...	1 (3.3)	1 (6.7)	0 (0)	.72
MSM	...	24 (80)	12 (80)	12 (80)	
Heterosexual	...	2 (6.7)	1 (6.7)	1 (6.7)	
Unknown	...	3 (10)	1 (6.7)	2 (13.3)	
AIDS diagnosis, no. (%)	...	4 (13.3)	3 (20)	1 (6.7)	.31
HIV RNA, median (IQR), log ₁₀ copies/mL	...	4.7 (4.4–5.2)	4.5 (4.2–5.5)	4.8 (4.4–5.2)	.85
CD4 ⁺ T-cell count, median (IQR), cells/ μ L					
Week 0 (ART naive)	...	250 (89–297)	234 (62–297)	262 (89–298)	.76
Week 48 (on ART)	...	415 (304–549)	416 (214–549)	398 (344–638)	.30
CD8 ⁺ T-cell counts, median (IQR), cells/ μ L					
Week 0 (ART naive)	...	878 (659–1156)	740 (658–1037)	1055 (648–1454)	.31
Week 48 (on ART)	...	857 (608–1414)	1168 (697–1414)	741 (567–1441)	.25
CD4/CD8 ratio, median (IQR), cells/ μ L					
Week 0 (ART naive)	...	0.21 (0.09–0.32)	0.20 (0.09–0.35)	0.22 (0.08–0.32)	.89
Week 48 (on ART)	...	0.43 (0.25–0.99)	0.32 (0.22–0.70)	0.65 (0.25–0.99)	.17
HCV coinfection, no. (%)	...	4 (13.3)	2 (13.3)	1 (6.7)	.54
Use of antibiotic in past 3 months, no. (%)	...	8 (26.7)	3 (20)	5 (33.3)	.41
First-line ART used, no. (%)					
INSTI based	...	17 (57)	9 (60)	8 (53.3)	.36
PI based	...	4 (13.3)	3 (20)	1 (6.7)	
NNRTI based	...	6 (40)	3 (20)	6 (40)	

Abbreviations: ART, antiretroviral therapy; BMI, body mass index; HCV, hepatitis C virus; HIV, human immunodeficiency virus; IDU, injection drug use; INRs, immune nonrecoverers; INSTI, integrase strand transfer inhibitor; IQR, interquartile range; IRs, immune recoverers; MSM, men who have sex with men; NNRTI, nonnucleoside reverse-transcriptase inhibitor; PI, protease inhibitor; SD, standard deviation.

^aBMI calculated as weight in kilograms divided by height in meters squared.

[7–14] per week in controls and 7 [4–10] in the HIV-infected group ($P = .02$).

Significant Impact of HIV and ART on Bacterial Richness and Diversity in Blood

Alpha diversity is used to measure the richness and evenness of bacterial taxa within a community. We found that, compared with controls, the blood microbiome of HIV-infected individuals showed a significantly higher alpha diversity using the Shannon index (richness and evenness) and Chao1 index (richness only). These differences were significantly attenuated after 48 weeks of ART, although ART-treated participants exhibited higher bacterial richness and diversity than controls (Figure 2A). Multidimensional scaling ordination (Supplementary Figure 2) and hierarchical clustering (Supplementary Figure 3) on beta diversity were performed for between-group comparisons based on the following 4 metrics: Bray-Curtis, Jaccard, UniFrac, and weighted UniFrac. The results showed no clear differences between groups at this structural level.

Graphic representations were made of the relative proportions of taxa for each taxonomic level (phylum, class, and order in Supplementary Figure 4, and family and genus in Figure 2B)

that were present in individual study samples. The blood was dominated by members of the families Pseudomonadaceae (*Pseudomonas*), Enterobacteriaceae, Comanodaceae, and Moraxellaceae (*Acinetobacter*) from the Proteobacteria phylum; the families Micrococcaceae (*Arthrobacter*) and Corynebacteriaceae (*Corynebacterium*) from Actinobacteria. From the Firmicutes phylum, we detected only, in low abundance, the Streptococcaceae family (*Streptococcus*). This bacterial signature is consistent with the composition of the blood microbiota previously described. The predominance of the Gammaproteobacteria class and Enterobacteriaceae families (Supplementary Figure 4) suggests that the intestinal lumen is a relevant source of these translocated bacteria.

The cladograms that were derived from the linear discriminative analysis effect size (LEfSe) analysis revealed that HIV-infected participants showed enrichment of Gammaproteobacteria (*Haemophilus*), Corynebacteriaceae (*Corinebacterium*), Microbacteriaceae (*Clavibacter*), and other bacterial orders, Lactobacillales, Bacillales and Rickettsiales, and depletion of Pseudomonadaceae (*Pseudomonas*) (Figure 2C). This pattern of dysbiosis was attenuated after 48 weeks of ART. Although we still found

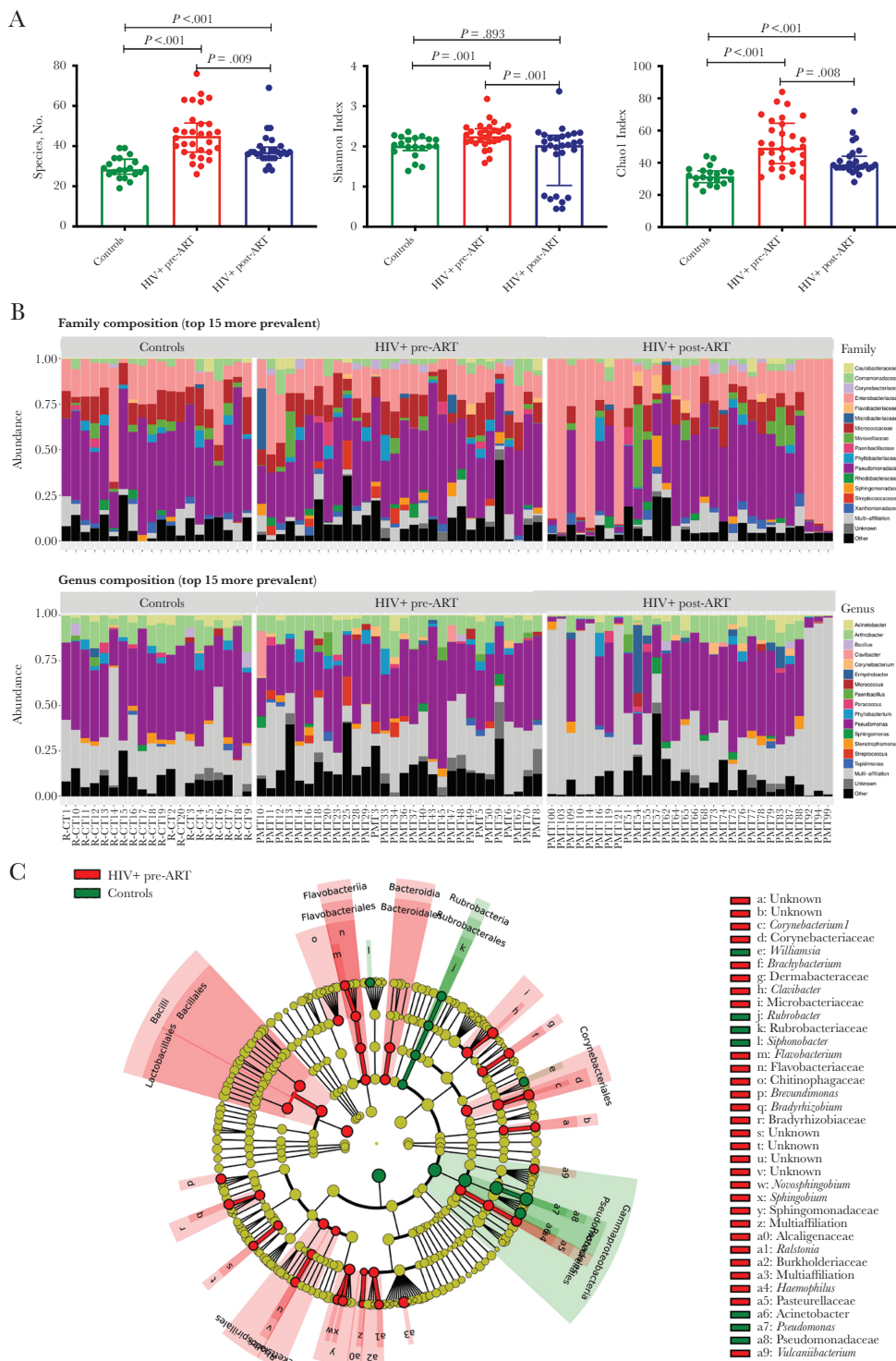


Figure 2. Bacterial microbiota structure in blood. *A*, Alpha diversity is used to measure the richness and evenness of bacterial taxa within a community. Richness is a simple measure and popular diversity index in ecology, where abundance data are often not available in the data sets of interest. The Chao1 index is considered a metric of the real richness since it estimates the number of taxa supported. The Shannon index is also a measure of the evenness (how evenly distributed the sequencing reads are among each taxa identified in each sample), and considers the number of different taxa and their abundance. Error bars represent median and interquartile ranges of the alpha diversity metrics in each group. Abbreviations: ART+, receiving antiretroviral therapy (ART), HIV+, HIV infected; naive, ART naive. *B*, Graphic representations of the relative proportion of taxa for family and genus levels present in individual study samples. Each bar represents the relative abundance of taxa in a single sample. Taxa are identified by name in the plot for the most abundant taxa. Taxa are merged into the "Other" category if less abundant. Taxa are merged into the "multiaffiliation" category when they can correspond to ≥ 2 different affiliations. Abbreviations: post-ART, after 48 weeks of ART; pre-ART, before ART. *C, D*, Linear discriminative analysis effect size (LEfSe) is an algorithm for high-dimensional biomarker discovery and explanation that can identify taxonomic groups, characterizing differences between ≥ 2 biological conditions. It emphasizes both statistical significance and biological relevance to identify differentially abundant features that are also consistent with biologically meaningful categories (subclasses). LEfSe first robustly identifies features that are significantly different among biological classes. The LEfSe result cladograms (genus and above levels) are shown for each analysis.

D

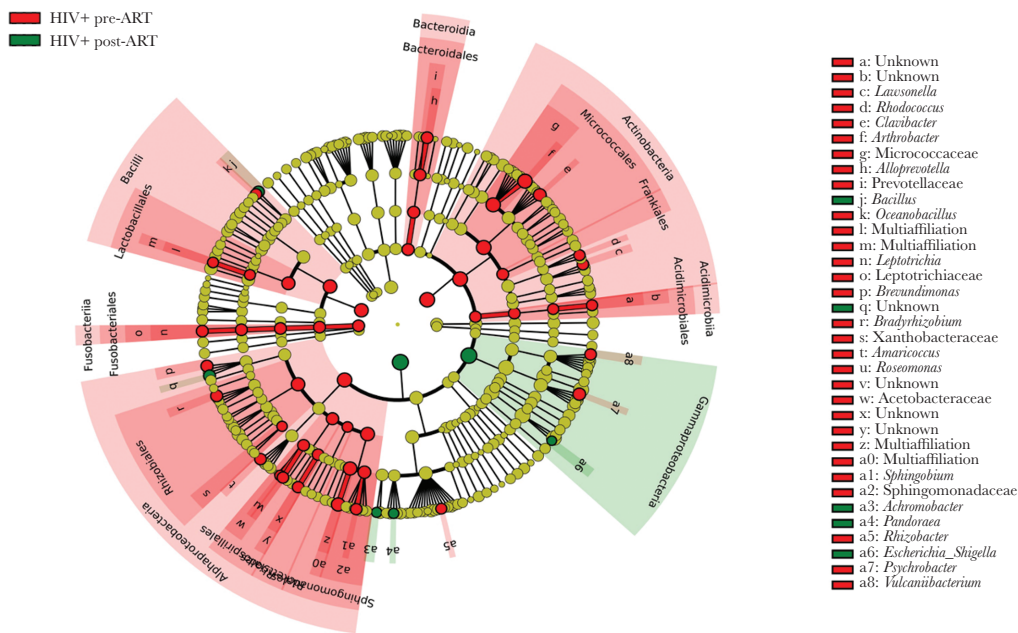


Figure 2. Continued.

enrichment for Gammaproteobacteria (*Escherichia-Shigella*) and Betaproteobacteria Achromobacter, Pandoraea) and depletion of Actinobacteria (Rubrobacteriaceae and Micrococaceae) (Figure 2D), these taxa were absent in the majority of samples.

ART Attenuation of Protein Translocation From Gut Bacteria

As shown above, HIV infection is associated with an increased translocation of bacteria from the gut to the blood. In that case, we would expect this increase to also be reflected in the number of proteins being translocated or synthesized by translocated bacteria. This information was obtained using a shotgun proteomic approach, in which we captured the expression profiles of proteins that were synthesized by bacteria in blood samples (Supplementary Table 1).

We first observed that the number of bacterial proteins with an expression level above the detection limit in blood was higher in HIV-infected individuals, especially before ART (mean [standard deviation], 5732 [169] proteins in healthy controls and 7292 [726] in the pre-ART HIV-infected group, and 6378 [1215] in the post-ART HIV-infected group) (Figure 3A). These differences are also appreciated considering the subset of 672 (healthy individuals), 907 (HIV infected, pre-ART), and 784 (HIV infected, post-ART) proteins that form the core proteome that represents individuals from each of the 3 groups. Thus, while HIV infection increases bacterial protein expression in the blood, ART attenuates this phenomenon. The bacterial protein expression profiles in blood identified an active microbiota structure,

with a predominance of the Firmicutes, Bacteroidetes, and Actinobacteria phyla. These taxonomic groups are also abundant components in stool samples, which strongly suggests that the source of these circulating bacterial proteins is the gut (Figure 3B).

Associations Between 16S Bacterial Sequences in Blood and Immune Recovery

While increased bacterial translocation is associated with adverse outcomes [3], it is unknown whether the nature of the translocated bacteria or by-products is functionally relevant and whether it affects the clinical course. Thus, we searched blood microbiota signatures that were associated with the extent of ART-mediated HIV-infected participants who were classified, based on the degree of immune recovery achieved after 48 weeks of ART, as *immune recoverers* (CD4/CD8 ratio fold change \geq p50) or *immune nonrecoverers* (CD4/CD8 ratio fold change $<$ p50). No statistically significant differences were observed in the general characteristics between groups (Supplementary Table 1). The groups differed, however, in several levels of biomarkers in blood. Immune recoverers showed a larger CD4/CD8 ratio at baseline, higher CD8⁺ T-cell activation, higher plasma CXCL10 levels, and lower plasma interleukin 10 levels.

The cladograms derived from LefSe analysis showed that before ART initiation, enrichment for the order of Lactobacillales and the families Nocardiaceae (*Rhodococcus*) and Flavobacteriaceae (*Flavobacterium*), and depletion of Moraxellaceae and Corynebacteriaceae families predicted

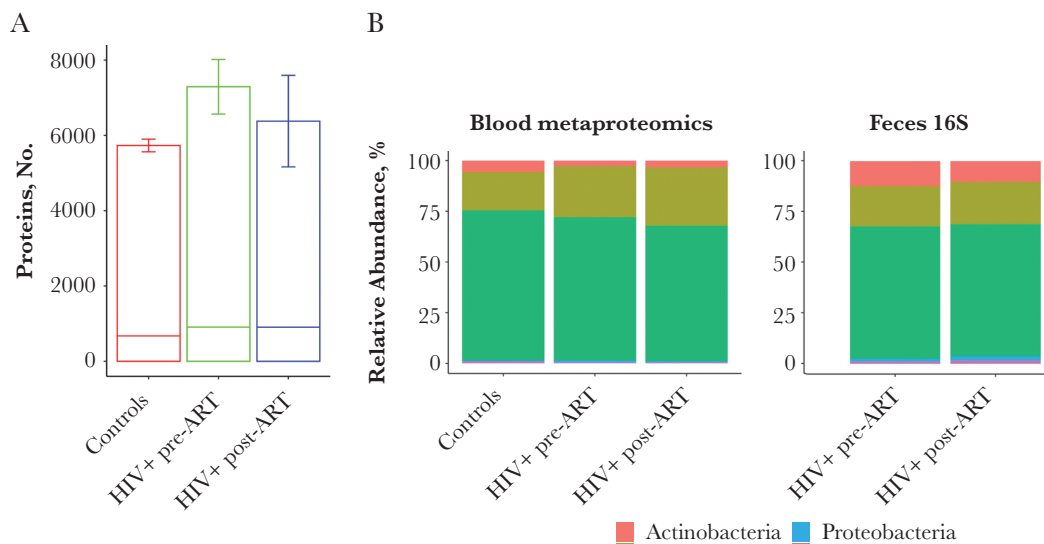


Figure 3. Bacterial protein signature in blood. *A*, Absolute number of bacterial proteins found to be expressed in group in each group. Bars represent the average number (mean with standard deviation) of proteins for all individuals. The horizontal line with each bar represents the number of proteins conforming the core proteome of each group, when considering common proteins of all individuals within each group. *B*, Microbiota composition at the phylum level derived from 16S sequences of fecal samples and from shotgun proteomic analysis of blood samples, in controls and in human immunodeficiency virus–infected (HIV+) participants. Note that fecal samples were available only in the HIV+ groups. Abbreviations: post-ART, after antiretroviral therapy; pre-ART, before antiretroviral therapy.

greater immune recovery after ART (Figure 4). To assess their possible implication in the pathogenesis of persistent immune dysfunction, we calculated the correlations between the whole community composition in blood and feces using correlation networks and the Benjamini-Hochberg correction, without evidence of a significant association (Supplementary Figure 5). Then, we selected the most enriched and depleted bacteria based on linear discriminative

analysis scores ≥ 2 from LefSe analysis, to be used in targeted correlation analyses with baseline levels and changes in relevant systemic biomarkers of clinical progression that were measured in plasma (soluble CD14 and CD163, C-reactive protein, lipoteichoic acid, tumor necrosis factor α , interleukin 6, 7, 10, and 17A, CXCL10) and peripheral blood mononuclear cells (percentage of HLA-DR⁺CD38⁺ CD8⁺ T cells).

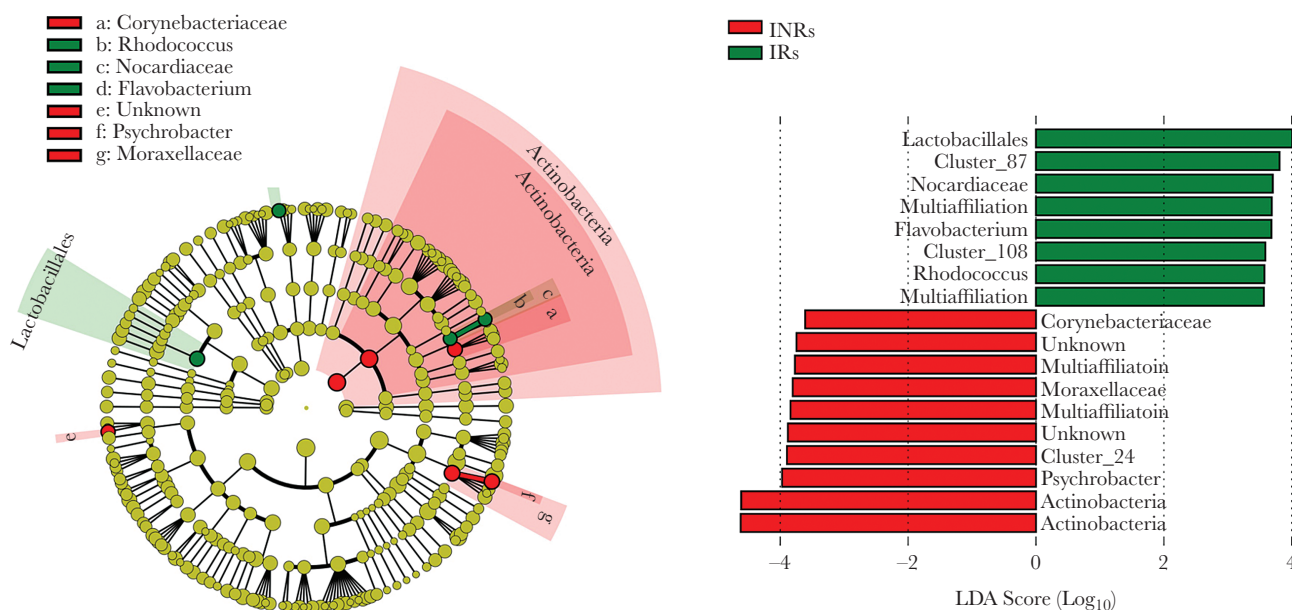


Figure 4. Microbial signature in blood associated to immune recovery. *A*, Cladogram of pairwise analysis of linear discriminative analysis (LDA) effect size (LEfSe) results for the comparison between immune recoverers (IRs) and immune nonrecovery (INRs). *B*, Bar plots of LEfSe analysis for the same comparison.

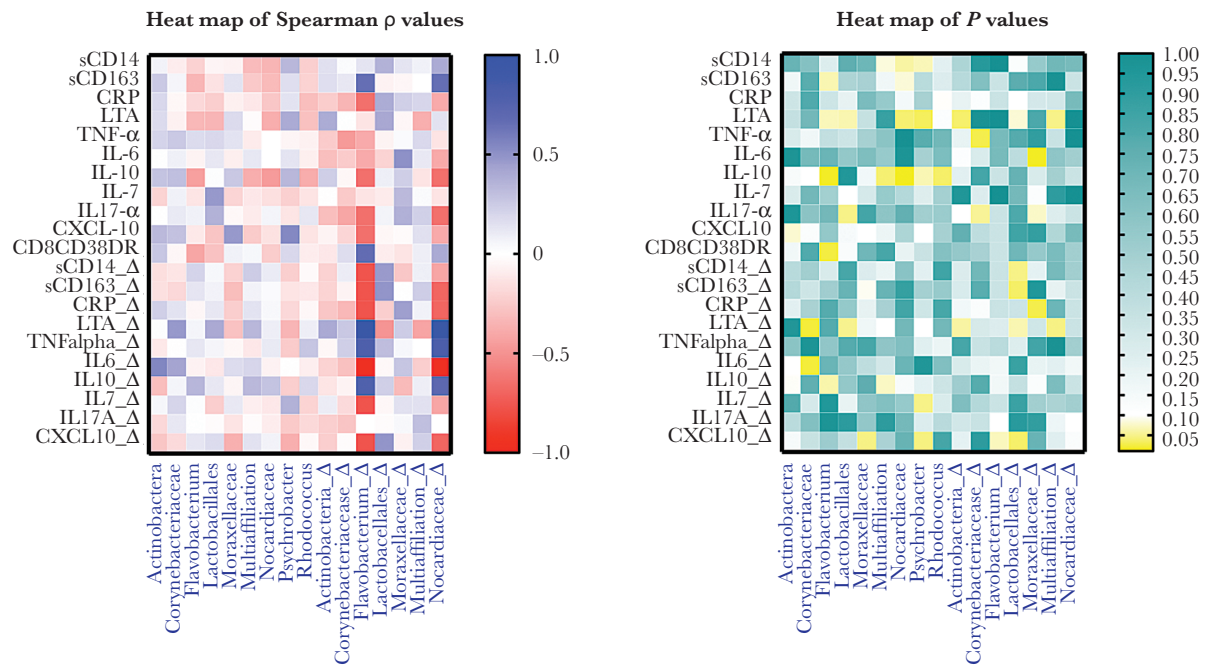


Figure 5. Heat map of targeted correlations between systemic biomarkers of disease progression and the taxa obtained from 16S sequences linked to antiretroviral therapy-mediated immune recovery according to linear discriminative analysis effect size analysis. We considered the baseline values of each parameter and their fold change (suffix “_Δ”) during the study period. *A*, Spearman ρ values. *B*, *P* values (not corrected for multiple comparisons). These biomarkers could not be measured in the control group owing to insufficient plasma volume. Abbreviations: CRP, C-reactive protein; IL-6 (etc), interleukin 6 (etc); LTA, lipoteichoic acid; sCD14, soluble CD14; sCD163, soluble CD163; TNF, tumor necrosis factor.

We found that baseline levels of these taxa or their changes during the study period were significantly correlated with the inflammation and immune activation biomarkers (Figure 5), reinforcing the concept that the nature of the translocated products influences ART-mediated immune recovery. To identify the associations that could be artificially driven by zero-inflated variable distributions, we visually examined the relative abundances in each group, revealing that *Nocardiaceae* family and *Rhodococcus* and *Flavobacterium* genera were absent in the majority of individuals (Supplementary Figure 6). Thus, the bacterial signature that was obtained from the circulating 16S rDNA and associated with immune recovery and inflammation included the class Actinobacteria, the Lactobacillales order, and the Corynebacteriaceae and Moraxellaceae families.

DISCUSSION

Because of the large number of studies demonstrating the persistence of structural and immunological defects in the GALT of HIV infection and the strong evidence showing that microbial translocation causes inflammation and drives disease progression [1–5], it is tempting to speculate that the nature of the translocated bacterial products may be affected by the GALT abnormalities caused by HIV infection. Conversely, the identity of the translocated products could affect HIV immunopathogenesis. In the current study, we investigated the identity of translocating bacteria in HIV-infected individuals.

We decided to recruit late-presenting HIV-infected individuals, to include a population with clear immunological harm secondary to HIV infection in which the potential associations between specific microbial signatures and the extent of immune recovery achieved during ART would be possible to evaluate. In our study, the overall bacterial signature according to 16S sequencing was dominated by members of the Gammaproteobacteria, Actinobacteria, and Bacteroidia classes, which is consistent with the dominant taxa found in the blood of healthy donors [22] and in European obese cohorts [31]. Taxonomic characterization from 16S sequences in plasma has been performed successfully in SIV-infected macaques [32].

The predominant phyla were dominated by Proteobacteria, followed by the Firmicutes, Tenericutes, and Bacteroidetes phyla [33]. In a different study in SIV-infected macaques, analysis of bacterial DNA that was isolated from the colon, liver, and mesenteric lymph nodes revealed a preference for the phylum Proteobacteria and an increased metabolic activity in Proteobacteria species within the colonic lumen, suggesting that Proteobacteria preferentially translocate [33]. Consistent with these observations, Proteobacteria was also the predominant phylum detected in the blood in our study for both control and HIV-infected groups, indicating commonalities in the mechanisms by which gastrointestinal bacteria translocate into the bloodstream between the SIV and HIV infection.

We found that HIV-infected individuals display a distinct microbial signature in the blood. This was already apparent at the alpha diversity level, indicating that HIV infection results in translocation of a larger repertoire of microorganisms compared with non-HIV-infected individuals. The greater bacterial richness and evenness were apparent before ART administration, arguing that the well-known beneficial immunological effects of suppressive ART also lead to attenuation of the blood microbiota dysbiosis that appear after HIV infection. We observed a specific bacterial signature of untreated HIV infection, with the presence of commensal bacteria that have with pathogenic potential observed only in immunosuppressed hosts (such as *Flavobacterium* genus, Chitinophagaceae family, and Lactobacillales order).

The potential origin of the bacteria deserves consideration. First, when approaching 16S rDNA sequencing data from blood samples, an initial possibility is that the detected bacteria originate from contamination at any step of blood samples and of many reagents are required for qPCR and sequencing procedures, which generates important methodological issues [34, 35]. Thus, contamination control was a critical step in our study. As explained in Methods, we followed standardized protocols to control contamination during DNA extraction in the qPCR experiments and searched for bacterial protein expression using a different technique.

In the case of contamination, a bacterial signature characteristic of a skin, water, or soil commensal would have been expected. While Proteobacteria can be found in their skin, their relative abundance compared with other phyla is low [36]. The predominance of the Gammaproteobacteria class and Enterobacteriaceae families (Supplementary Figure 4) is consistent with a gastrointestinal signature that indicates a gastrointestinal origin of the translocated bacteria from the gut, as described elsewhere [32]. The finding of the associated microbial signatures for each group argues against this possibility, because bacterial contamination should have equally affected all study groups if this was the case. A second consideration concerns the significance of the findings. We used a DNA extraction technique from whole blood that was able to extract the DNA also from circulating T cells. Thus, we cannot infer from the 16S sequencing analysis whether the signal originated from free DNA fragments, DNA in living, dormant, or degraded bacteria, circulating DNA, or DNA inside human cells.

To gain insight into the functional relevance of these findings, we profiled the blood metaproteomes in each group of samples (controls; HIV infected, pre-ART; and HIV infected, post-ART). The blood microbiota composition was annotated from the bacterial proteins that were correlated with the fecal microbiota profiles obtained from 16S sequencing analysis. This finding indicates that the bacterial proteins that are translocated into the blood could originate from the gut or from viable bacteria trafficking from the gut. Thus, ART decreased the number of bacterial proteins found in the HIV-infected group,

reinforcing the idea that the immunological improvement obtained after 48 weeks of ART results in a normalization of the translocated bacterial proteins. This may most likely be caused by the restoration of the intestinal mucosa after ART.

Because we studied HIV-infected late presenters who were at greater risk of inadequate immune recovery after ART [37], a relevant question is whether these microbial products that were specifically translocated in HIV-infected individuals are relevant for HIV immunopathogenesis. We found that enrichment of Lactobacillales and depletion of Actinobacteria, Corynebacteriaceae, and Moraxellaceae were significantly associated with greater immune recovery after ART. In addition, these taxa were correlated with the inflammatory markers measured in plasma and the T-cell activation markers measured in blood mononuclear cells (Figure 4), which suggests that the molecular cross talk between the host and the translocated bacterial products could influence ART-mediated immune recovery.

The fact that the Lactobacillales family, which includes mucosal-adherent and lactic-acid producers, was the most significantly associated taxon with ART-mediated immune recovery reinforces the biological relevance of our results. A previous cross-sectional study in HIV-infected individuals found a predominance of plasma enterobacterial DNA among immune nonrecoverers compared with immune recoverers [38], in contrast to that found in children with HIV [39]. In another longitudinal study in immune nonrecoverers and immune recoverers, bacterial plasma amplification was performed using standard PCR precautions to avoid contamination, and, in keeping with our findings, immune recoverers were found enriched in members of the Lactobacillaceae family [40].

The main strengths of our study are the novelty of the data. This is, to the best of our knowledge, the first characterization of the blood microbiota in HIV-infected individuals using a combined approach of next-generation metagenomic sequencing with a thorough control of contamination and validation by shotgun proteomics and the longitudinal follow-up of the study participants, which allowed to assess the effect of 48 weeks of ART on study outcomes.

Our study has some limitations, including the existence of potential sources of bias, such as diet or sexual orientation or the higher frequency of men in the HIV-infected group compared with the control group, which could have affected the results, in contrast to the studies in SIV-infected macaques [32, 41]. The lack of matching by risk factors that could have influenced the microbiome, such as diet, sex, sexual orientation, or use of medications is a source of potential bias that could have affected the comparison between patients and healthy individuals. In addition, sampling gut biopsy specimens, with obvious practical and ethical constraints, would have allowed us to visualize translocating bacteria to clarify the mechanisms driving the greater predisposition of certain microbial products to translocate during HIV infection and identify the gastrointestinal site

from which the bacterial products translocated. A reasonable possibility is that the bacterial products do not translocate from the colon, where the abundance of Proteobacteria is relatively low, but instead translocate from the small intestine, where the percentage of Proteobacteria is comparatively higher [41].

In summary, a hallmark of advanced HIV infection is greater diversity of translocated microbial products, which likely originated through the metabolic activity of the gut bacteria. ART ameliorates this blood dysbiosis at the structural and functional level, but the identity of the translocated products seems to affect the extent of ART-mediated immune recovery and the presence of systemic inflammation. Deciphering the cross talk between the host and the microbial bacteria that translocate from the gut would lay the groundwork for designing new strategies for HIV-infected individuals who have suboptimal immune recovery despite suppressive ART.

Supplementary Data

Supplementary materials are available at *The Journal of Infectious Diseases* online. Consisting of data provided by the authors to benefit the reader, the posted materials are not copyedited and are the sole responsibility of the authors, so questions or comments should be addressed to the corresponding author.

Notes

Acknowledgments. The authors acknowledge all the study participants who contributed to this work as well as the clinical research staff who made this research possible. They also acknowledge Sergio Ciordia, who performed shotgun proteomic analysis at the Proteomics Facility of the Spanish National Center for Biotechnology, ProteoRed, PRB3-ISCIII.

Authors' contributions. S. S. V. and M. F. conceptualized the study. S. S. V., S. S. C., A. T. R., B. L., F. S., and M. J. G. analyzed the data and generated the figures. C. G., A. V., and N. M. measured the markers of inflammation and immune activation. B. L., F. S., and M. J. G. performed the 16S ribosomal RNA gene sequencing experiments and bioinformatic analyses, B. L. and F. S. in blood samples and M. J. G. in fecal samples. S. S. C. and M. F. performed the proteomic experiments and bioinformatic analyses. S. S. V., J. I. B., V. E., O. B., M. d. L., J. M. S., R. R., S. H., and S. M. contributed to data mining and recruitment of study participants. S. S. V. wrote the first draft of the manuscript, and all authors revised and approved the final manuscript.

Financial support. This work was supported by the Instituto de Salud Carlos III (Plan Estatal de I+D+i 2013–2016, projects PI15/00345 and PI18/00154); the Fundación Asociación Española Contra el Cáncer within the European Research Era-NET aligning national/regional translational cancer research programs and activities program (grant AC17/00019) and cofinanced by the European Development Regional Fund; and Plan Estatal de I+D+i 2013–2016 (grant PT17/0019 to

the Proteomics Facility of the Spanish National Center for Biotechnology).

Potential conflicts of interest. Outside the submitted work, S. S. V. reports personal fees from ViiV Healthcare, Janssen Cilag, Gilead Sciences, and Merck Sharp & Dohme (MSD) as well as nonfinancial support from ViiV Healthcare and Gilead Sciences and research grants from MSD and Gilead Sciences. B. L. and F. S. work for Vaiomer. All other authors report no potential conflicts. All authors have submitted the ICMJE Form for Disclosure of Potential Conflicts of Interest. Conflicts that the editors consider relevant to the content of the manuscript have been disclosed.

References

1. Brenchley JM, Price DA, Schacker TW, et al. Microbial translocation is a cause of systemic immune activation in chronic HIV infection. *Nat Med* **2006**; 12:1365–71.
2. Estes JD, Harris LD, Klatt NR, et al. Damaged intestinal epithelial integrity linked to microbial translocation in pathogenic simian immunodeficiency virus infections. *PLoS Pathog* **2010**; 6:e1001052.
3. Sandler NG, Douek DC. Microbial translocation in HIV infection: causes, consequences and treatment opportunities. *Nat Rev Microbiol* **2012**; 10:655–66.
4. Brenchley JM, Douek DC. The mucosal barrier and immune activation in HIV pathogenesis. *Curr Opin HIV AIDS* **2008**; 3:356–61.
5. Zevin AS, McKinnon L, Burgener A, Klatt NR. Microbial translocation and microbiome dysbiosis in HIV-associated immune activation. *Curr Opin HIV AIDS* **2016**; 11:182–90.
6. Somsouk M, Estes JD, Deleage C, et al. Gut epithelial barrier and systemic inflammation during chronic HIV infection. *AIDS* **2015**; 29:43–51.
7. Jiang W, Lederman MM, Hunt P, et al. Plasma levels of bacterial DNA correlate with immune activation and the magnitude of immune restoration in persons with antiretroviral-treated HIV infection. *J Infect Dis* **2009**; 199:1177–85.
8. Sandler NG, Wand H, Roque A, et al; INSIGHT SMART Study Group. Plasma levels of soluble CD14 independently predict mortality in HIV infection. *J Infect Dis* **2011**; 203:780–90.
9. Tenorio AR, Zheng Y, Bosch RJ, et al. Soluble markers of inflammation and coagulation but not T-cell activation predict non-AIDS-defining morbid events during suppressive antiretroviral treatment. *J Infect Dis* **2014**; 210:1248–59.
10. Mudd JC, Brenchley JM. Gut mucosal barrier dysfunction, microbial dysbiosis, and their role in HIV-1 disease progression. *J Infect Dis* **2016**; 214(suppl 2):S58–66.
11. Mavigner M, Cazabat M, Dubois M, et al. Altered CD4+ T cell homing to the gut impairs mucosal immune reconstitution in treated HIV-infected individuals. *J Clin Invest* **2012**; 122:62–9.

12. Vujkovic-Cvijin I, Dunham RM, Iwai S, et al. Dysbiosis of the gut microbiota is associated with HIV disease progression and tryptophan catabolism. *Sci Transl Med* **2013**; 5:193ra91.
13. Dinh DM, Volpe GE, Duffalo C, et al. Intestinal microbiota, microbial translocation, and systemic inflammation in chronic HIV infection. *J Infect Dis* **2015**; 211:19–27.
14. Vázquez-Castellanos JF, Serrano-Villar S, Latorre A, et al. Altered metabolism of gut microbiota contributes to chronic immune activation in HIV-infected individuals. *Mucosal Immunol* **2015**; 8:760–72.
15. Serrano-Villar S, Rojo D, Martínez-Martínez M, et al. Gut bacteria metabolism impacts immune recovery in HIV-infected individuals. *EBioMedicine* **2016**; 8:203–16.
16. Pandrea IV, Gautam R, Ribeiro RM, et al. Acute loss of intestinal CD4⁺ T cells is not predictive of simian immunodeficiency virus virulence. *J Immunol* **2007**; 179:3035–46.
17. Gordon SN, Klatt NR, Bosinger SE, et al. Severe depletion of mucosal CD4⁺ T cells in AIDS-free simian immunodeficiency virus-infected sooty mangabeys. *J Immunol* **2007**; 179:3026–34.
18. Potgieter M, Bester J, Kell DB, Pretorius E. The dormant blood microbiome in chronic, inflammatory diseases. *FEMS Microbiol Rev* **2015**; 39:567–91.
19. Antinori A, Coenen T, Costagiola D, et al; European Late Presenter Consensus Working Group. Late presentation of HIV infection: a consensus definition. *HIV Med* **2011**; 12:61–4.
20. GESIDA/PNS. Guidelines for the use of antiretroviral agents in HIV-infected adults. **2016**. <https://www.msssi.gob.es/ciudadanos/enfLesiones/enfTransmisibles/sida/publicaciones/profSanitarios/docTARGesidaPNS2013Def.pdf>.
21. Lluch J, Servant F, Païssé S, et al. The characterization of novel tissue microbiota using an optimized 16S metagenomic sequencing pipeline. *PLoS One* **2015**; 10:e0142334.
22. Païssé S, Valle C, Servant F, et al. Comprehensive description of blood microbiome from healthy donors assessed by 16S targeted metagenomic sequencing. *Transfusion* **2016**; 56:1138–47.
23. Schierwagen R, Alvarez-Silva C, Servant F, Trebicka J, Lelouvier B, Arumugam M. Trust is good, control is better: technical considerations in blood microbiome analysis. *Gut* **2020**; 69:1362–3.
24. Anhê FF, Jensen BAH, Varin TV, et al. Type 2 diabetes influences bacterial tissue compartmentalisation in human obesity. *Nat Metab. Nature Research* **2020**; 2:233–42.
25. Salter SJ, Cox MJ, Turek EM, et al. Reagent and laboratory contamination can critically impact sequence-based microbiome analyses. *BMC Biol* **2014**; 12:87.
26. Laurence M, Hatzis C, Brash DE. Common contaminants in next-generation sequencing that hinder discovery of low-abundance microbes. *PLoS One* **2014**; 9:e97876.
27. Nadkarni MA, Martin FE, Jacques NA, Hunter N. Determination of bacterial load by real-time PCR using a broad-range (universal) probe and primers set. *Microbiology* **2002**; 148:257–66.
28. Escudié F, Auer L, Bernard M, et al. FROGS: find, rapidly, OTUs with galaxy solution. *Bioinformatics* **2018**; 34:1287–94.
29. Ruiz-Ruiz S, Sanchez-Carrillo S, Ciordia S, et al. Functional microbiome deficits associated with ageing: chronological age threshold. *Aging Cell* **2020**; 19:e13063.
30. Rosting C, Gjelstad A, Halvorsen TG. Water-soluble dried blood spot in protein analysis: a proof-of-concept study. *Anal Chem* **2015**; 87:7918–24.
31. Lelouvier B, Servant F, Païssé S, et al. Changes in blood microbiota profiles associated with liver fibrosis in obese patients: a pilot analysis. *Hepatology* **2016**; 64:2015–27.
32. Ericson AJ, Lauck M, Mohns MS, et al. Microbial translocation and inflammation occur in hyperacute immunodeficiency virus infection and compromise host control of virus replication. *PLoS Pathog* **2016**; 12:e1006048.
33. Klase Z, Ortiz A, Deleage C, et al. Dysbiotic bacteria translocate in progressive SIV infection. *Mucosal Immunol* **2015**; 8:1009–20.
34. Ferri E, Novati S, Casiraghi M, et al. Plasma levels of bacterial DNA in HIV infection: the limits of quantitative polymerase chain reaction. *J Infect Dis* **2010**; 202:176–8.
35. Svärd J, Sönnernborg A, Vondracek M, Mölling P, Nowak P. On the usefulness of circulating bacterial 16S rDNA as a marker of microbial translocation in HIV-1-infected patients. *J Acquir Immune Defic Syndr* **2014**; 66:87–89.
36. Oh J, Byrd AL, Deming C, Conlan S, Kong HH, Segre JA; NISC Comparative Sequencing Program. Biogeography and individuality shape function in the human skin metagenome. *Nature* **2014**; 514:59–64.
37. Woo KS, Chook P, Yu CW, et al. Effects of diet and exercise on obesity-related vascular dysfunction in children. *Circulation* **2004**; 109:1981–6.
38. Marchetti G, Bellistri GM, Borghi E, et al. Microbial translocation is associated with sustained failure in CD4⁺ T-cell reconstitution in HIV-infected patients on long-term highly active antiretroviral therapy. *AIDS* **2008**; 22:2035–8.
39. Fitzgerald FC, Lhomme E, Harris K, et al; CHAPAS-3 Trial Team. Microbial translocation does not drive immune activation in Ugandan children infected with HIV. *J Infect Dis* **2019**; 219:89–100.
40. Merlini E, Bai F, Bellistri GM, Tincati C, d'Arminio Monforte A, Marchetti G. Evidence for polymicrobial flora translocating in peripheral blood of HIV-infected patients with poor immune response to antiretroviral therapy. *PLoS One* **2011**; 6:e18580.
41. Klase Z, Ortiz A, Deleage C, et al. Dysbiotic bacteria translocate in progressive SIV infection. *Mucosal Immunol* **2015**; 8:1009–20.